

Provided for non-commercial research and education use.
Not for reproduction, distribution or commercial use.



This article appeared in a journal published by Elsevier. The attached copy is furnished to the author for internal non-commercial research and education use, including for instruction at the authors institution and sharing with colleagues.

Other uses, including reproduction and distribution, or selling or licensing copies, or posting to personal, institutional or third party websites are prohibited.

In most cases authors are permitted to post their version of the article (e.g. in Word or Tex form) to their personal website or institutional repository. Authors requiring further information regarding Elsevier's archiving and manuscript policies are encouraged to visit:

<http://www.elsevier.com/copyright>



Contents lists available at ScienceDirect

Earth and Planetary Science Letters

journal homepage: www.elsevier.com/locate/epsl

Origin and stability of a permafrost methane hydrate occurrence in the Canadian Shield

Randy L. Stotler^{a,*}, Shaun K. Frapè^a, Lasse Ahonen^b, Ian Clark^c, Shane Greene^c, Monique Hobbs^{d,1}, Elizabeth Johnson^{e,2}, Jean-Michel Lemieux^f, Richard Peltier^g, Lisa Pratt^e, Timo Ruskeeniemi^b, Ed Sudicky^a, Lev Tarasov^h^a Department of Earth and Environmental Sciences, University of Waterloo, 200 University Ave. West, Waterloo, ON, Canada N2L 3G1^b Geological Survey of Finland, Espoo, Finland^c Department of Earth Sciences, University of Ottawa, Ottawa, ON, Canada^d Nuclear Waste Management Organization, Toronto, ON, Canada^e Department of Geological Sciences, Indiana University, Bloomington, Indiana, USA^f Département de géologie et de génie géologique, Université Laval, Québec, QC, Canada^g Department of Physics, University of Toronto, Toronto, ON, Canada^h Department of Physics and Physical Oceanography, Memorial University of Newfoundland, St. John's, Newfoundland, Canada

ARTICLE INFO

Article history:

Received 25 March 2009

Received in revised form 11 May 2010

Accepted 20 May 2010

Available online 18 June 2010

Editor: M.L. Delaney

Keywords:

methane hydrate
climate change
continental glaciation
permafrost
thermogenic gas
Canadian Shield

ABSTRACT

Relatively little attention has been given to the stability of methane hydrates, formed during periods of past climate change, currently in areas of continuous permafrost. Although a large portion of the Canadian arctic is underlain by crystalline rocks, the occurrence, phase, and origin of alkanes in crystalline rocks under thick permafrost conditions (>500 m) have not been reported. For the first time, composition and isotopic data for gases from a crystalline shield environment currently under permafrost conditions are presented. Gas and water samples were collected from exploration boreholes and seeps between 890 and 1130 m depths in the Lupin gold mine, Nunavut, Canada. Gases were methane-dominant (64–87%), with nitrogen (10–37%) the next largest component, and smaller amounts of ethane, propane, and carbon dioxide. Pressure and temperature measurements indicated gas hydrates were stable at the site prior to mining operations, a conclusion supported by noble gas and salinity determinations. Gas hydrate stability over the last 120 kyr glacial cycle was demonstrated by calculating transient subsurface pressure and temperature conditions utilizing the *Memorial University/University of Toronto Glacial Systems Model* (MUN/UofT GSM) and the *Hydrogeosphere* groundwater flow model. Model results also indicated glacial loading increased subsurface pressures, resulting in increased hydrate stability fields during glacial periods. Subglacial groundwater recharge would be limited by any significant formation of gas hydrates. Gas composition, combined with carbon and hydrogen isotopic determinations on methane (–56 to –42‰ VPDB and –349 to –181‰ VSMOW), carbon dioxide (–55 to –15‰ VPDB), ethane (–37 to –27‰ VPDB and –330 to –228‰ VSMOW), and propane (–34 to –27‰ VPDB and –196 to –172‰ VSMOW), indicated formation of natural gases by thermogenic processes, mixed with bacteriogenic gas, reasonable, given site geologic history. Methane hydrate formation affected gas composition and gas $\delta^2\text{H}$ values, complicating the interpretation. Gas production is not a modern process at this location, and the overall contribution to the global carbon budget is small. Glacial groundwater recharge models need to account for methane hydrate formation and dissipation due to changes in subsurface stability fields during glaciation and the effect of methane hydrate on hydraulic conductivity.

© 2010 Elsevier B.V. All rights reserved.

1. Introduction

Gas-hydrates form under certain low temperature and medium pressure conditions, when water and gas mixtures crystallize into ice-like solids, storing >160 times more gas per unit-volume than free gas (Sloan, 1998). It has been suggested that melting of methane hydrates added significant quantities of greenhouse gases to the atmosphere during past periods of climate change, primarily due to destabilization of marine hydrate reservoirs (e.g. Kennett et al., 2000). Although the

* Corresponding author. Now at: Kansas Geological Survey, University of Kansas, USA. Tel.: +1 785 864 2096; fax: +1 785 864 5317.

E-mail address: stotler@kgs.ku.edu (R.L. Stotler).

¹ Now at: Institute of Geological Sciences, University of Bern, Switzerland.

² Now at: University of Tennessee, USA.

permafrost methane hydrate reservoir is considered to be several orders of magnitude smaller than the marine reservoir, large occurrences of thermogenic (with bacteriogenic components) alkane and methane-hydrate have been found in permafrost-affected sedimentary rocks, occurring in the Arctic Archipelago and Mackenzie Delta in Canada, the North Slope Basin in Alaska, and Siberia (Collett et al., 1990; Dallimore and Collett, 1995, 2005; Dallimore et al., 1999; Yakushev and Chuvilin, 2000; Kvenvolden and Lorenson, 2001; Majorowicz and Osadetz, 2001). Methane is formed through three natural processes: (1) thermogenically, from thermal decomposition of organic matter; (2) bacteriogenically, from methanogenic microbes; and (3) abiogenically, when CO₂ reduces to CH₄ through non-biological reactions, and are typically differentiated based on the ratio of different gas components and their respective isotopic compositions (e.g. Sackett et al., 1970; James, 1983; Whiticar et al., 1986; Prinzhofer and Huc, 1995; Whiticar, 1999; McCollom and Seewald, 2001, 2007). Recent investigations have indicated that during methane hydrate formation, both the ratio of different gases in a given sample, and their respective hydrogen isotopic compositions, can change, possibly affecting interpretations of gas origin and evolution (Milkov et al., 2004; Hatchikubo et al., 2007; Hachikubo et al., 2009). Studies of methane-hydrates have focused on oil- and gas-producing regions, which are concentrated in existing marine and sedimentary basins. As such, there is currently no information available regarding the nature of gas associated with crystalline shields in permafrost environments.

Field activities at the Lupin gold mine (65°45′29″N, 111°13′10″W), a metamorphosed amphibolite-grade banded-iron-formation within an Archean metaturbidite sequence in Nunavut, Canada, provided an opportunity to study the nature of gases within crystalline shield rocks in a permafrost environment (Fig. 1). Field studies were conducted towards the end of 23-years of mine operations. Today, Lupin is well within the continuous permafrost zone; permafrost depth, defined by the 0 °C isotherm, varied between 400 and 600 m in the area. Mineshaft temperature measurements by mine officials indicated permafrost depth (541 m) remained unchanged during mine operations. However, subsurface pressure conditions were affected due to mine dewatering that extended to depths of 1500 m, necessitating investigation and understanding of the mine's affect on physical and chemical systems (Stotler et al., 2009). In this study, we used a 3D glacial systems model to examine how glacial and periglacial conditions affected methane hydrate stability through the last (Wisconsin) glacial cycle in the Lupin region. Origin and evolution of the gas was also examined to relate this particular gas occurrence with other gas and gas hydrate deposits. The combination of the above analyses constrains the relative contribution of methane hydrate in crystalline shields to the global carbon budget during past climate change, and allows investigation into the influence methane hydrate formation has to understanding gas occurrence origins and evolution in this type of terrain.

2. Methods

Water and gas samples were collected between 250 and 1300 m below ground surface (mbgs) from fractures, dripping exploration boreholes, and packer-sealed research boreholes. Natural gas was identified between 890 and 1130 mbgs. Gas samples were collected from one fracture pool, nine sub-horizontal and three sub-vertical research boreholes. Samples were analyzed for gas chemistry, $\delta^{13}\text{C}$ and $\delta^2\text{H}$ composition of the gases, dissolved ions, and $\delta^{18}\text{O}$ and $\delta^2\text{H}$ composition of the water. The boreholes were generally drilled across steeply dipping foliation and away from mine workings for lengths from 60 to 500 m. They were sealed with 3 m Margot[®] packers, allowing pressure to build up within the boreholes. One borehole was sampled on the 890 mbgs level, and eleven on the 1130 mbgs level. Three research boreholes were also drilled just

beneath the base of the permafrost at the 550 and 570 mbgs levels, however no gas was observed in samples collected from these boreholes. The eleven boreholes on the 1130 mbgs level allow investigation of hydraulic conditions over a planar area of 500 m × 500 m, with the total distance between borehole collars about 300 m. Additionally, one borehole was drilled 500 m down, and one 30 m up. Fractures and fracture zones were mapped in each borehole under un-pressurized conditions using a borehole camera. Gas was readily observed effervescing from several fracture openings in each borehole.

Noble gas samples were collected at in situ pressures via two different methods: copper tubes and a gas diffusion sampler. In the copper tube method, three copper tubes were connected in series to the boreholes. Ball valves and pressure gauges were used to control flow and maintain formation water pressure at both the water inlet and outlet. After flushing for 1–2 h, flow was reduced and pressure allowed to recover before each copper tube was clamped and sealed at each end with pinch-off tools to create a cold weld seal. The second method entailed use of a gas diffusion sampler, modified for the high pressures. The sampler was constructed of a stainless steel chamber with eight holes through the body. Silica tubing, filled with silica glass beads to prevent crushing by water pressure connected six of the holes through the chamber. Six copper tubes 13–14 cm long pinched and soldered on the distal end to provide an air-tight seal were attached to the outside of the sampling chamber to the ports connected by silica tubing. The two remaining ports to the sample chamber were used for water flow in and out of the chamber. Once attached to the borehole, sampling operates in a similar fashion as with the copper tube method. The sampler is flushed for 24 h and flow reduced. When samples were ready, pinch off tools were utilized to create a cold weld seal along the copper tube near the sample chamber.

The Indiana University Stable Isotope Facility and the University of Waterloo (UW) Environmental Isotope Laboratory analyzed $\delta^{13}\text{C}$ and $\delta^2\text{H}$ isotopes using Micromass Isoprime GC–C–IRMS for carbon isotopes and Finnigan MAT Delta GC–PYR–IRMS for hydrogen isotopes. Accuracy and reproducibility of $\delta^{13}\text{C}$ and $\delta^2\text{H}$ are typically $\pm 0.3\%$ VPDB and $\pm 5\%$ VSMOW, respectively. Gas compositions were analyzed at the UW Organic Geochemistry Laboratory; N₂ and CO₂ on a Fisher/Hamilton Gas Partitioner, Model 29 gas chromatograph, and alkane-hydrocarbons on a Varian 3800 gas chromatograph equipped with a flame ionization detector and capillary injection port. Detection limits for CO₂, N₂, C₁, C₂, C₃, nC₄ and iC₄ are 0.5 ppm, 30 ppm, 0.3 µg/L, 0.2 µg/L, 0.2 µg/L, 0.8 µg/L, and 1.6 µg/L, respectively. Noble gas concentrations were measured at the University of Ottawa using an isotope dilution method (Youngman, 1989). Methane ¹⁴C analyses were prepared and analyzed at IsoTech Laboratories.

Bulk organic carbon was determined at Indiana University by acidifying the sample with 1 N HCl for 1 h at 55 °C, then filtered and a fraction loaded into baked ceramic crucibles for analysis via an ELTRA C/S elemental analyzer. Difference in organic carbon content for duplicate rock samples ranged from 0.01% to 0.05%, and was similar in reproducibility to analytical standards which varied by less than 0.03% for the six replicates combusted during this study.

The climate/subsurface modeling results are from a large ensemble calibration of the Memorial University/University of Toronto (MUN/UofT) *Glacial Systems Model* (GSM) for the last glacial cycle. The model includes a 3-D thermo-mechanically coupled ice-sheet model, permafrost resolving bed thermal model, diagnostic surface drainage, visco-elastic bedrock response, and positive degree day surface mass-balance module (Tarasov and Peltier, 2007). The eight model runs presented are a hand-picked set of high-scoring runs that roughly bound possible climate ranges. It should be noted that model results prior to the last glacial maximum are poorly constrained due to limited data. Detail of climate forcing and the calibration can be found in Tarasov and Peltier (2005).

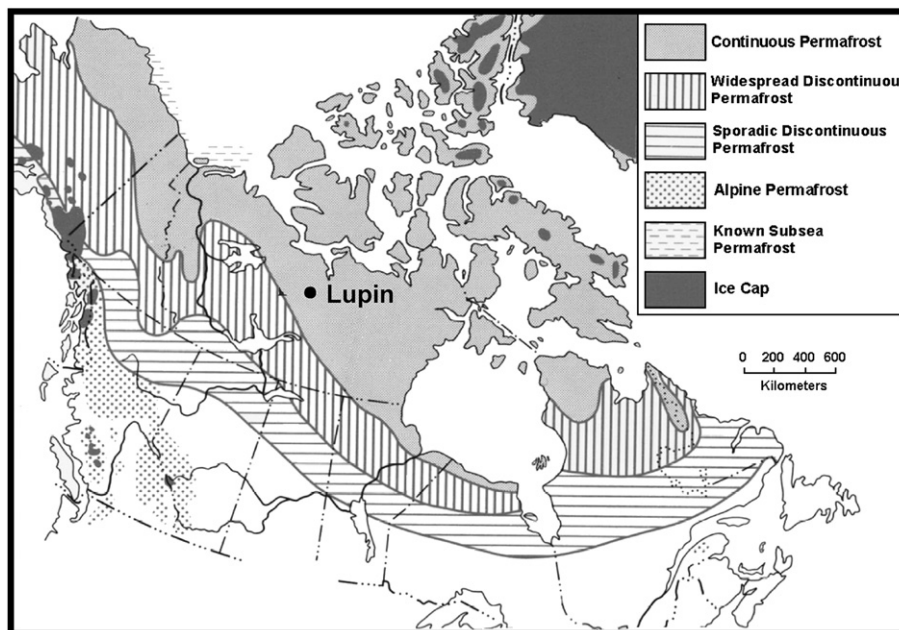


Fig. 1. Location of Lupin in relation to permafrost zones (after Natural Resources Canada, 1995).

The pressure-melting point of gas-hydrates was determined by utilizing a best fit of previously compiled data (Sloan, 1998). For temperatures above 0 °C this relationship is defined by: $T(P) = 9.0416 \cdot \ln(P/2492.6)$; and for temperatures below 0 °C: $T(P) = 30.338 \cdot \ln(3.917 \cdot 10^{-4}P)$, where T = temperature [°C] and P = pressure [kPa].

Transient subsurface hydraulic conditions were modeled, accounting for density-dependent groundwater flow, hydromechanical ice-sheet loading, brine evolution, subglacial infiltration, relative sea level variations, isostasy, and permafrost development using the *Hydrogeosphere* model (Therrien et al., 2007), and applied to the Wisconsinan glaciation over the entire Canadian landscape using one GSM output as input boundary conditions. Further details concerning the model configuration may be found in Lemieux et al. (2008a,b,c).

3. Results and discussion

Gas was produced from all boreholes sampled on the 1130 and 890 m levels. Gas produced varied between 0.09 $L_{\text{gas}}/L_{\text{H}_2\text{O}}$ of water to

0.50 $L_{\text{gas}}/L_{\text{H}_2\text{O}}$ (Table 1). Certain boreholes (1130-217 and 1130-260) were observed to produce significantly more gas than fluid prior to being sealed. Gas production was only observed by borehole video from certain fractures (see Supplementary Fig. 1).

As there were multiple sampling events at each sampling location, a summary of the Lupin gas molecular and isotopic compositions may be found in Tables 1 and 2, with complete datasets available with the Supplementary data. Gases were generally methane-dominated (64–87%), with nitrogen as the next largest component (10–37%), and smaller amounts of ethane, carbon dioxide, and propane. Very small amounts of butane and iso-butane were detected in most samples. Methane and carbon dioxide carbon isotopic compositions varied between –56 and –42‰ (VPDB) and –55 and –15‰ (VPDB), respectively. A smaller range was detected for ethane (–37 to –27‰ VPDB) and propane (–34 to –27‰ VPDB). However, methane hydrogen isotopes showed a smaller range (–349 to –330‰ VSMOW) than ethane (–312 to –228‰ VSMOW), but similar to propane (–196 to –172‰ VSMOW). The small concentration of butane precluded hydrogen isotopic composition analysis.

Table 1
Summary of molecular gas compositions sampled at Lupin. Noble gas data from Greene (2005).

Sample ID	Ne	He·10,000	Ar	Kr	Xe	N ₂	CO ₂	C ₁	C ₂	C ₃	i-C ₄	n-C ₄	C ₁ C ₂ + C ₃	Gas vol. (L) 1 L water
	$\frac{[(CC_{\text{gas}}/CC_{\text{H}_2\text{O}})_{\text{sample}}]}{[(CC_{\text{gas}}/CC_{\text{H}_2\text{O}})_{0^\circ\text{C}_{\text{equilibrium}}]}}$					(vol.%)								
890-188	2.4	3.8	2.5	1.4	1.5	28.5	0.47	74.4	0.55	0.014	ND	0.0002	132	0.09
1130-64	NA	NA	NA	NA	NA	36.9	0.14	64.4	0.11	0.004	0.000	0.0001	565	
1130-160	NA	NA	NA	NA	NA	NA	NA	69.6	2.40	0.169	NA	NA	55	
1130-175	NA	NA	NA	NA	NA	9.63	1.67	86.7	1.89	0.094	0.007	0.007	44	
1130-176	NA	NA	NA	NA	NA	11.0	1.42	84.7	1.60	0.089	0.008	0.007	50	
1130-NED-Pool	NA	NA	NA	NA	NA	26.9	0.98	72.6	1.09	0.002	0.003	0.003	66	
1130-191	5.6	20.0	5.9	1.1	1.4	15.8	1.38	81.1	1.49	0.080	0.004	0.004	52	0.33
1130-192	4.1	5.9	10.5	0.4	0.5	11.0	1.92	86.7	2.05	0.124	0.006	0.006	40	0.50
1130-197 ¹	2.8	11.3	4.2	1.3	1.4	22.7	0.88	77.4	0.93	0.033	0.001	0.001	80	0.20
1130-217	3.0	6.7	4.3	0.9	1.2	15.1	1.43	81.5	1.61	0.083	0.004	0.004	48	0.27
1130-219	1.1	4.0	3.1	0.6	0.8	16.2	1.17	82.2	1.27	0.046	0.001	0.001	62	0.14
1130-267	NA	NA	NA	NA	NA	27.5	0.79	69.5	0.93	0.037	0.002	0.002	80	
1130-273	NA	NA	NA	NA	NA	13.9	1.32	81.8	1.42	0.068	0.004	0.005	55	

Table 2
Summary of gas isotopic compositions sampled at Lupin.

Sample ID	$\delta^2\text{H}$ (VSMOW)			$\delta^{13}\text{C}$ (VPDB)			
	C ₁	C ₂	C ₃	C ₁	C ₂	C ₃	CO ₂
	(‰)			(‰)			
890-188	-340	-253	-189	-56.1	-36.7	-33.5	-21.9
1130-64	-330	ND	ND	-50.3	-27.3	-27.3	-55.3
1130-160	-323	-276	-172	-46.1	-34.9	-33.2	-26.4
1130-175	-328	-290	-179	-44.3	-34.5	-33.3	-18.6
1130-176	-344	-243	ND	-44.7	-35.7	-32.3	ND
1130-NED-Pool	-329	-312	ND	-47.3	-32.8	ND	ND
1130-191	-319	-305	ND	-47.1	-34.9	-33.1	-21.1
1130-192	-324	-295	-196	-42.4	-35.0	-34.2	-23.0
1130-197 ¹	-341	-281	-183	-50.6	-35.3	-33.2	-24.3
1130-217	-337	-308	ND	-45.2	-36.6	ND	ND
1130-219	-349	-228	ND	-47.7	-35.5	ND	ND
1130-267	-344	-290	-179	-47.8	-35.0	-33.6	-21.1
1130-273	-344	-289	-178	-46.3	-34.3	-32.9	-15.7

3.1. Physical nature of Lupin gas

Due to the presence of methane gas in a region affected by thick permafrost, the potential for gas-hydrate formation was considered. Short of visibly observing methane hydrate, identification of methane hydrate is difficult, often resulting in a debate over the presence or absence of hydrate. This is even the case in areas where significant quantities of methane are extracted (e.g. Collett and Ginsburg, 1998). After over thirty years of research, direct gas quantification of methane in marine hydrates has only recently been achieved at two sites (Dickens et al., 1997; Milkov et al., 2003). Geophysical techniques, such as seismic surveys to identify a “bottom simulating reflector” often associated with hydrate occurrences, have been utilized in sedimentary and marine units to identify gas hydrates (e.g. Milkov et al., 2003; Tréhu et al., 2004); however such surveys were not available at Lupin.

Gas quantity estimates at Lupin were averaged over the length of each borehole, because gas quantification in individual fractures was not possible. This distinction is noteworthy; down-hole video logging clearly indicated that gas was produced only from certain fractures (see Supplementary information). Therefore, with fluid produced from most of the fractures, and gas only from some, the average gas concentration measured from the borehole is less than the amount in individual gas producing fractures. At Lupin, it was not possible to physically measure gas quantities within individual fractures.

Gas hydrate stability is determined by thermal and pressure conditions. Measured temperatures (8–13 °C) and hydrostatic pressures (8725–11,078 kPa) at the sampling depths were within the gas-hydrate stability field (Fig. 2), indicating that given a large enough quantity of gas, the area surrounding the mine is conducive to gas-hydrate formation. The immediate area of the Lupin mine was drained (depressurized) to a depth of approximately 1500 mbgs during mining. In-situ pressures measured along the 400 m-long tunnel at borehole collars had a significant range (1550–5930 kPa) (Fig. 2). As indicated by the difference between in situ and hydrostatic pressures, the observed mine-induced depressurization would cause dissipation of methane hydrates in fractures located near the mine or intersected by the drilled boreholes.

The hypothesis that pressures in gas-producing fractures were closer to hydrostatic pressure than the measured *in situ* pressure is supported by noble gas data. Low concentrations of Ne, Kr, and Xe relative to air-equilibrated water (Fig. 3A and B) indicate a post-equilibrium process affected gas partial pressures. Gas equilibria in fluids are described by Henry's law; temperature, pressure, and salinity all affect gas solubility (e.g. Mazor, 1972; Kipfer et al., 2002). Generally, decreasing pressure or temperature, or increasing salinity, will result in decreasing gas solubilities, although the relative impact

to individual noble gases varies (e.g. Kipfer et al., 2002). Compared with Ne, both Kr and Xe are significantly more sensitive to changes in temperature (e.g. Mazor, 1972). However, concentrations of Ne, Kr, and Xe are all lower than expected (Fig. 3A and B) and no relationship with salinity was observed (Greene, 2005). Therefore, significant depressurization of the rock and water in fractures encountered by the boreholes explain the observed noble gas separation (Greene, 2005).

When pressure decreases within boreholes (during drilling or when opened for sampling), methane hydrate dissociation is expected to cause a decrease in both temperature and salinity (Hesse and Harrison, 1981; Sloan, 1998; Wright et al., 1999; Tréhu et al., 2004). Substantial differences in measured salinity (2.2 g l⁻¹ and 40 g l⁻¹) and temperatures (7.5–13.4 °C) were observed between eleven parallel boreholes sampled along a 400 m-long tunnel. Water temperatures varied over five years of study by more than 2.2 °C in five of the boreholes, with a maximum variation of 3.5 °C (Fig. 4, Supplementary data). Over the period of study, fluid temperatures were observed to decrease after drilling, until the boreholes were sealed (Fig. 4, Supplementary data). Fluid temperatures then increased, unless the boreholes were allowed to depressurize (Fig. 4). Temperatures decreased in the one borehole that was not able to be sealed completely (1130-267, Fig. 4). Differences were also observed during sampling and between samplings in individual boreholes. During one experiment, several boreholes were allowed to completely depressurize over two days. Temperature decreased by up to 2 °C,

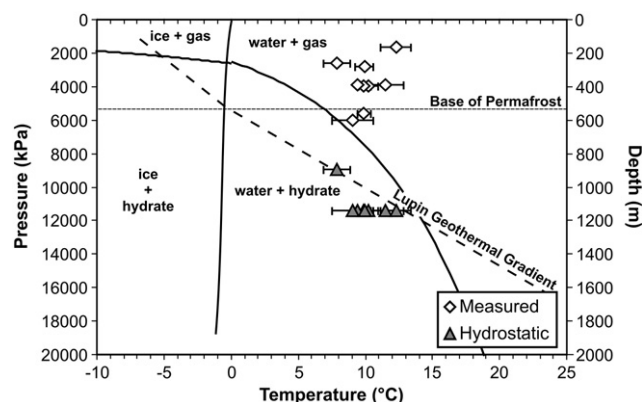


Fig. 2. Gas-hydrate stability fields at Lupin. Pressure–temperature fields for boreholes sampled at the 890 and 1130 m levels, with a conservative geothermal gradient. Maximum and minimum recorded temperatures are represented by the error bars. Under hydrostatic conditions, gas hydrates are stable, but depressurization near the mine results in dissociation of gas hydrates, as shown by measured pressures.

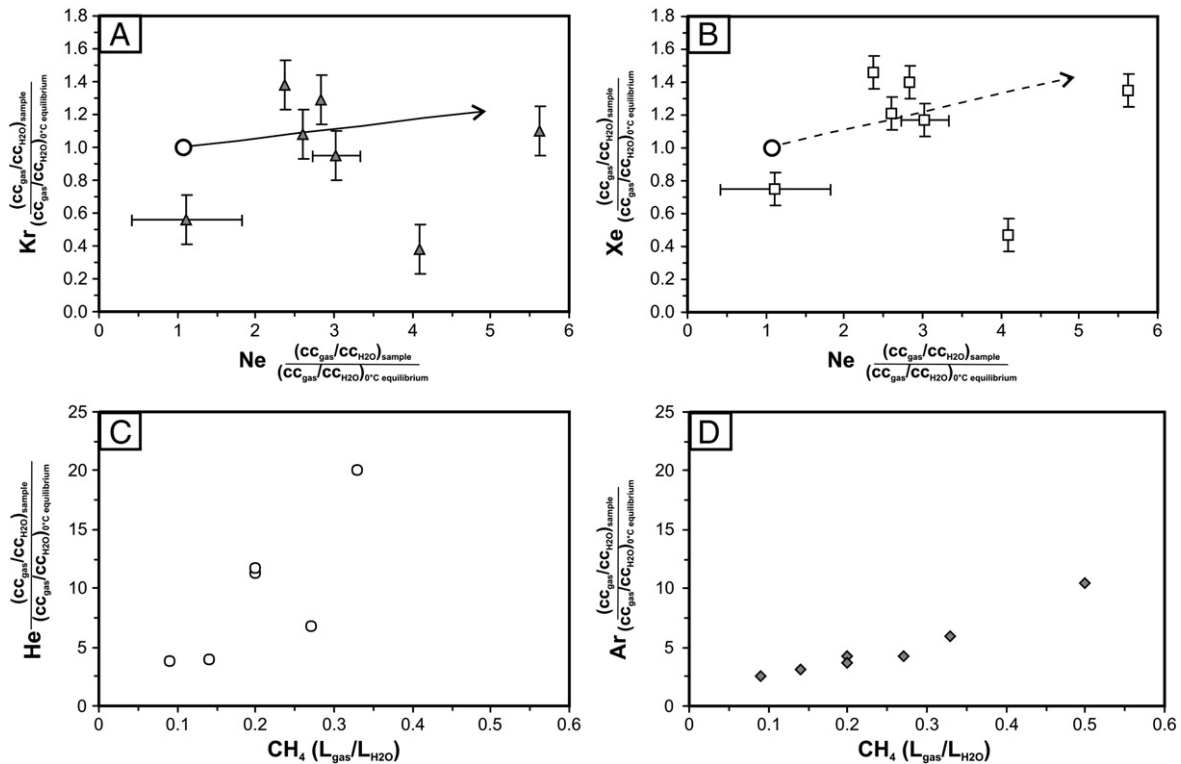


Fig. 3. Results of noble gas analyses from samples collected at the Lupin mine, with all noble gas concentrations displayed as sample concentration normalized to fresh water concentrations at 0 °C. (A) Kr and (B) Xe versus Ne, with the expected increased excess air trends with respect to Kr (solid line) and Xe (dashed line). Unlike Ar and He, the noble gases Ne, Kr, and Xe are largely unaffected by subsurface sources and in-situ production, with concentrations established from atmospheric concentrations and gas solubility during recharge (Kipfer et al., 2002). Displacement of samples below the excess air line is believed to be indicative of depressurization within the rock mass. Correlation of (C) He*10,000 and (B) Ar versus methane. Modified from Greene (2005).

while electrical conductivity decreased by up to 300 mS/m. These changes in temperature are within the range observed (2–5 °C) during gas hydrate dissociation in both the laboratory and the field (Wright et al., 1999; Zhou et al., 2009). All of the trends described are consistent with the presence of methane hydrates, providing evidence that methane hydrates are present in the rock distally from the mine. Mixing of different fluids from various fracture networks could also

explain heterogeneous temperature and salinity values. However, the systematic variation of these values within all of the boreholes (a majority drilled parallel to each other across the rock foliation), while varying directly with changes in pressure, in a small area, is considered strong evidence to indicate the presence of methane hydrate.

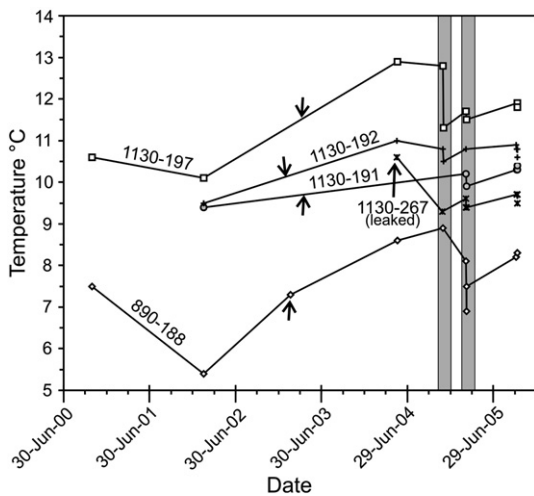


Fig. 4. Borehole temperature variation for select Lupin boreholes. Arrows indicate date boreholes were sealed. 1130-267 was sealed incompletely and leaked. All boreholes on the diagram except 267 were drilled in the 1990s. Grey shaded areas indicate periods when temperature measurements were taken before and after borehole depressurization. Temperatures clearly declined during these periods in each of the boreholes. The final set of temperature measurements were taken at static conditions.

3.2. Glacial influence on gas hydrate stability

Evidence suggests methane hydrate releases occurred during Quaternary interstadials (Nisbet, 1990; Kennett et al., 2000). Therefore, hydrate stability at Lupin over the last 120 kyr was evaluated. The effect of the glacial cycle to hydrate stability was examined with a combination of GSM and hydraulic modeling. Eight estimates of hydrate stability using subsurface temperature and pressure calculations were derived from a glacial systems model with different reconstructions spanning possible climate ranges (Fig. 5). Up to four glacial advances and retreats are predicted to have affected the site over the last 120 kyr (Fig. 5). Although permafrost stability fields are typically reduced during glaciation by warm subglacial temperatures (e.g. Tarasov and Peltier, 2007), the GSM results indicate gas hydrate stability fields actually increased. This is corroborated by hydraulic modeling of subglacial conditions, which suggests increased hydrostatic pressure from glacial loads dominate over subglacial warming in controlling gas hydrate stability (Fig. 6, Lemieux et al., 2008a). All simulations suggest gas hydrates have remained stable at the sampling depths, even in scenarios where permafrost melted completely beneath the glaciers. Importantly, in permafrost areas such as Lupin, methane release to the atmosphere would be unlikely throughout much of the glacial cycle, since a core area of methane hydrate remains stable.

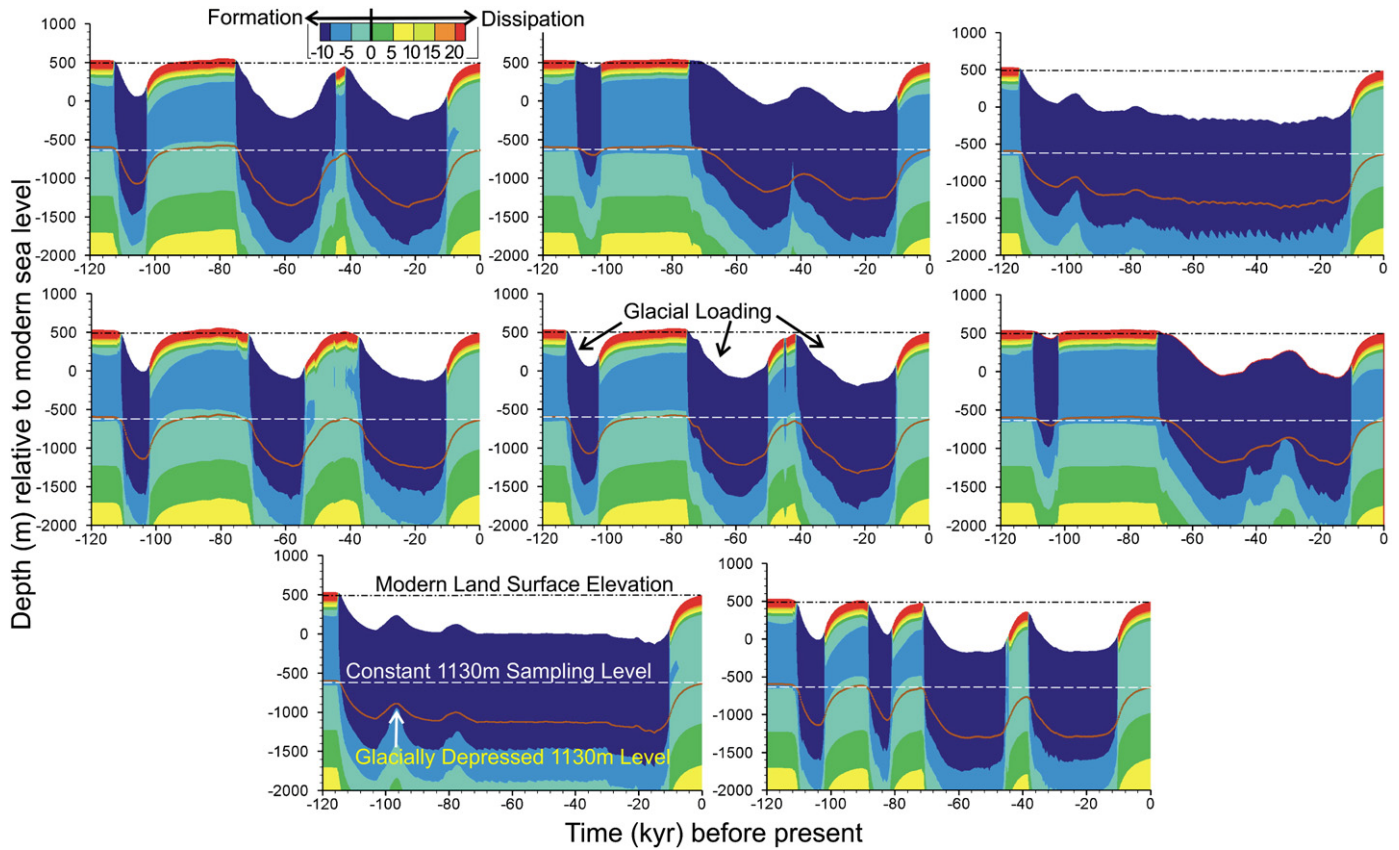


Fig. 5. Results of glacial systems modeling of eight different climate scenarios. Contours show temperature with respect to methane hydrate pressure melting point over the last 120 kyr at Lupin. Contours below zero indicate hydrate stability. Elevation (left axis) is shown with respect to modern sea level (0 m). The changing land surface elevation due to isostatic loading and unloading of glacial ice is depicted, and the black dash-dot line represents modern land surface elevation unaffected by glacial loading. The 1130 m sampling depth is shown with respect to both the modern land surface (dashed white line) and the isostatic land surface (solid red line).

While Nisbet (1990) indicated that glacial melting and pressure release would result in gas hydrate destabilization, with subsequent release of CO₂ and CH₄ to the atmosphere, it is also important to consider the effect of gas hydrate formation during glacial onset, and continued stability in permafrost areas throughout the glacial cycle. Previously, Weitemeyer and Buffett (2006) suggested subglacial methane hydrate formation could occur as a result of methanogenesis of the shallow soil organic carbon pool. However, with the exception of these investigations, the potential importance of subglacial hydrates has received very little attention. The results presented in

this paper indicate that hydrate could form at much greater depths beneath a glacier.

The potential for methane hydrate formation also affects the current understanding of subglacial fluid flow. Current groundwater flow models account for numerous transient conditions (see list in methods sections), but do not account for the presence of methane (Person et al., 2007; Lemieux et al. (2008a,b,c)). Methane hydrates reduce porosity and permeability similar to ice (e.g. Burt and Williams, 1976; Kleinberg et al., 2003). Thus even when permafrost melts under a “warm-footed” glacier, a substantial increase in porosity and permeability beneath a glacier would not necessarily occur if methane hydrates were present or formed as a result of glaciation. The potential for deep subglacial recharge in areas with significant methane hydrate accumulations would be limited. This demonstrates the need to understand the entire physical system, including the state of the gaseous system, when evaluating subglacial meltwater recharge to aquifers.

3.3. Origin and evolution of the gas

Although modeling suggests the methane at Lupin has been stable throughout the recent glacial cycles, understanding the origin, relative age, and evolution of the gas phase is pertinent to understanding the importance to the global carbon budget should the gas hydrates dissociate at a future time. Further, there have been recent suggestions that methane hydrate formation can affect gas molecular and isotopic compositions (Milkov et al., 2004; Hatchikubo et al., 2007; Hachikubo et al., 2009). Crystalline shield gases have previously been reported to be of abiogenic or bacteriogenic origins (Voytov, 1991; Sherwood Lollar et al., 1993a,b, 2002, 2006; Potter et al., 2004), and

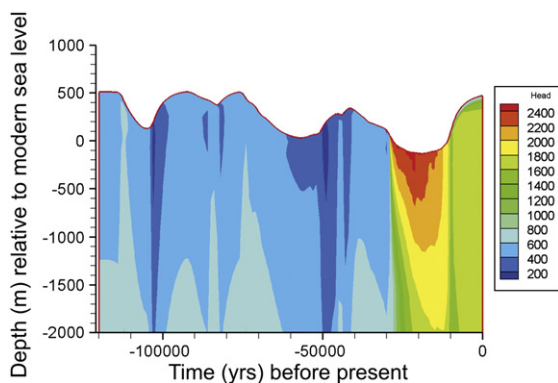


Fig. 6. Subsurface hydraulic conditions predicted by *Hydrogeosphere* over the last 120 kyr at Lupin, Nunavut. In the modeled scenario, permafrost melted completely only during the last glacial advance, drastically increasing subsurface hydraulic pressures. Hydraulic head is shown in m.

this discussion will help determine what, if any, affect gas hydrate formation may have on the interpretations of origin and evolution of these gases.

3.3.1. Gas origin

Trends in relative abundance combined with isotopic composition are widely used to identify thermogenic gas reservoirs and to differentiate thermogenic from bacteriogenic and abiogenic hydrocarbon gases (e.g. Sackett et al., 1970; Whiticar et al., 1986; Prinzhofer and Huc, 1995; McCollom and Seewald, 2007). As gas is thermogenically formed, higher hydrocarbons are thermally cracked, resulting in a low (<100) methane (C_1) to ethane plus propane ($C_2 + C_3$) ratio, where lighter isotopes are preferentially removed from longer chain hydrocarbons, resulting in more negative $\delta^{13}C$ values for C_1 than for higher hydrocarbons such as C_2 or C_3 (e.g. Prinzhofer and Huc, 1995; Whiticar, 1996). Bacteriogenic gas forms from carbonate reduction or methyl-fermentation, with little to no higher hydrocarbons forming, and therefore has a high $C_1/(C_2 + C_3)$ ratio (>1000) (Whiticar et al., 1986; Oremland et al., 1988; Whiticar, 1999; Hinrichs et al., 2006). A -75% fractionation occurs between the carbon source (typically CO_2 or acetate) and the resulting methane, with typical bacteriogenic $\delta^{13}C-CH_4$ values more depleted than -60% VPDB (e.g. Claypool et al., 1985; Whiticar et al., 1986; Whiticar, 1999). A range of empirical relationships comparing δ^2H-H_2O and $-CH_4$ have also been published to identify bacterially-mediated methanogenic pathways, as specific proportion of hydrogen atoms are incorporated into methane from water molecules along different pathways (e.g. Schoell, 1980; Jenden and Kaplan, 1986; Whiticar et al., 1986; Waldron et al., 1999; Whiticar, 1999).

Recent experimental work strongly suggests caution is warranted when using carbon isotopes to differentiate abiogenic synthesis from other hydrocarbon sources; as a result, determination of abiogenic gas formation and subsequent fractionation is still the subject of investigation and debate (McCollom and Seewald, 2006, 2007; Taran et al., 2007). Empirical data show abiogenic gases generally evolve a low $C_1/(C_2 + C_3)$ ratio (<100), similar to thermogenic gases, but with progressively more negative $\delta^{13}C$ values as hydrocarbon chains get longer (i.e. from C_1 towards C_3), often described as a “reversed isotopic trend” (e.g. Des Marais et al., 1981; McCollom and Seewald, 2007; Taran et al., 2007). This isotopic trend is not unique to abiogenic gas formation however (McCollom and Seewald, 2007; Taran et al., 2007). It has been suggested that when gases are observed with a “reversed isotopic trend” in conjunction with hydrocarbon 2H values significantly more negative than thermogenic (-430% to -230%), an abiogenic origin may be ascribed (Sherwood Lollar et al., 2002, 2006; McCollom and Seewald, 2007).

These typical isotopic interpretation methods provided conflicting information about the origin of gases sampled at Lupin. The gases had low $C_1/(C_2 + C_3)$ values (Fig. 7A), a trait common to both thermogenic and abiogenic gas. The enrichment trend of $\delta^{13}C$ from C_1 to C_3 alkanes is typical of thermogenic gas (Fig. 7B), and is opposite from the “reversed isotopic trends” typically ascribed to a number of different processes including abiogenic gas formation (McCollom and Seewald, 2007). However, a bacteriogenic methyl-type fermentation origin for the gas is consistent with the most depleted methane δ^2H and $\delta^{13}C$ values (Fig. 7C), and the relationship between δ^2H-CH_4 and $-H_2O$ in the Lupin gas (Fig. 8A) is indicative of bacteriogenic carbonate reduction methanogenesis utilizing modern δ^2H-H_2O values (-190 to -170% VSMOW). Mixing of two different methane gas sources was indicated by the wide range of $\delta^{13}C-C_1$ values and the relationship between the $C_1/(C_2 + C_3)$ and $\delta^{13}C-C_1$ values (Fig. 7A). This pattern is typically interpreted as mixing between a ^{13}C depleted ($<-65\%$ VPDB), high $C_1/(C_2 + C_3)$ ratio (>1000) bacteriogenic end-member and a relatively ^{13}C enriched ($>-35\%$ VPDB), low $C_1/(C_2 + C_3)$ ratio (<100) thermogenic end-member. A more comprehensive analysis considering the relationship of fractionation

between both $\delta^{13}C$ and δ^2H for C_1 , C_2 , and C_3 was consistent with gas of a thermogenic origin (Fig. 7D), where both $\delta^{13}C$ and δ^2H become isotopically heavier from C_1 to C_2 to C_3 (e.g. Sherwood Lollar et al., 1994; Prinzhofer and Huc, 1995). This pattern does not follow previously recognized abiogenic gas trends (Des Marais et al., 1981; Sherwood Lollar et al., 2002, 2006; McCollom and Seewald, 2007; Taran et al., 2007). H_2 , required for most abiogenic methane reactions (McCollom and Seewald, 2007), was present only in low concentrations at Lupin (Onstott et al., 2009), further arguing against an abiogenic origin for Lupin gases.

A thermogenic gas origin at Lupin is reasonable given the geologic history of the area. About 2.8 Ga, the central Slave structural province was part of a marine accretionary margin and subject to proto-plate tectonic forces (Kusky, 1989). At Lupin, amphibolite facies metamorphism (low-pressure and high-temperature) from multiple intrusions and metamorphic events (peaking 2.68–2.585 Ga) altered turbidite mudstones and greywackes to the crystalline rock types meta-greywacke/quartzite, phyllite and quartz-feldspar-gneiss (King et al., 1988; Geusebroek and Duke, 2004). Proterozoic faulting (1.84–1.81 Ga), resulting in contact metamorphism, is the last dated metamorphic event in the area (Geusebroek and Duke, 2004). The thermogenic gas component was likely derived from the regional metamorphic alteration of marine sediments (turbidites) into metaturbidites and amphibolitic gneisses. Organic carbon content at Lupin range between 0.02 and 0.99 wt.%, averaging 0.27 wt.%. Thus adequate carbon was available for thermogenic alteration. The original gases were generated and trapped in the meta-sediments during metamorphism. Graphitic carbon ($\delta^{13}C$: -22.62 and -27.1% VPDB) on fractures and bedding surfaces is a common occurrence in Lupin rock samples, with visible large graphite veins, and is an inferred remnant of previously migrating hydrocarbon fluids. Bituminous rocks and oil-rich fluid inclusions are found at other sites in the Canadian Shield, indicating formation of thermogenic gases from Archean and Paleoproterozoic units was feasible (Petersilie and Sørensen, 1970; Goodarzi et al., 1992; Mossman et al., 1993; Melezhik et al., 1999; Dutkiewicz et al., 2003).

It is possible that some of the gases were formed during bacteriogenic carbonate reduction. While the δ^2H-CH_4 values are more depleted than typically found for bacteriogenic carbonate reduction methanogenesis, similar depleted δ^2H values have been observed in methane emissions from Arctic lakes (Whiticar et al., 1986; Walter et al., 2008). The lowest $\delta^{13}C-C_1$ value (-56% VPDB) was not as ^{13}C depleted as typical for bacteriogenic gas ($<-60\%$ VPDB). However, in a previous study of Lupin calcite isotopic composition, with fluid inclusion filling temperatures between 160 and 270 °C, some abnormally enriched $\delta^{13}C$ values ($+30\%$ VPDB) in hydrothermal calcite were found, indicating an enriched source of $\delta^{13}C-CO_2$ (Stotler et al., 2009). Methane fluid inclusions were also observed in the calcite (Stotler et al., 2009). Given the typical $\delta^{13}C$ fractionation of $\sim -77\%$ between CH_4 and CO_2 for methane produced by bacteriogenic carbonate reduction (e.g. Claypool et al., 1985), such an enriched $\delta^{13}C-CO_2$ source could result in $\delta^{13}C-C_1$ values as high as -45% (VPDB), within the range of the most depleted Lupin $\delta^{13}C-C_1$ values. Similar $\delta^{13}C-CO_2$ and $\delta^{13}C-CH_4$ values were found in the Middle America Trench, an analogous modern environment (Claypool et al., 1985). Thus a bacteriogenic carbonate reduction source is not unreasonable for the most ^{13}C depleted Lupin gas end-member. But, this would almost certainly require the sampled methane to have been generated at the same time as the calcites, since modern gas $\delta^{13}C-CO_2$ values (typically -26 to -15% VPDB) were much more negative than the $+30\%$ VPDB required to produce bacteriogenic gas with the observed values. It is therefore unlikely that a bacteriogenic gas component is currently being produced.

Additional evidence supports a non-modern source for any bacteriogenic gas component. Methanogenic bacteria were not isolated at the site (Onstott et al., 2009), and fluid redox conditions

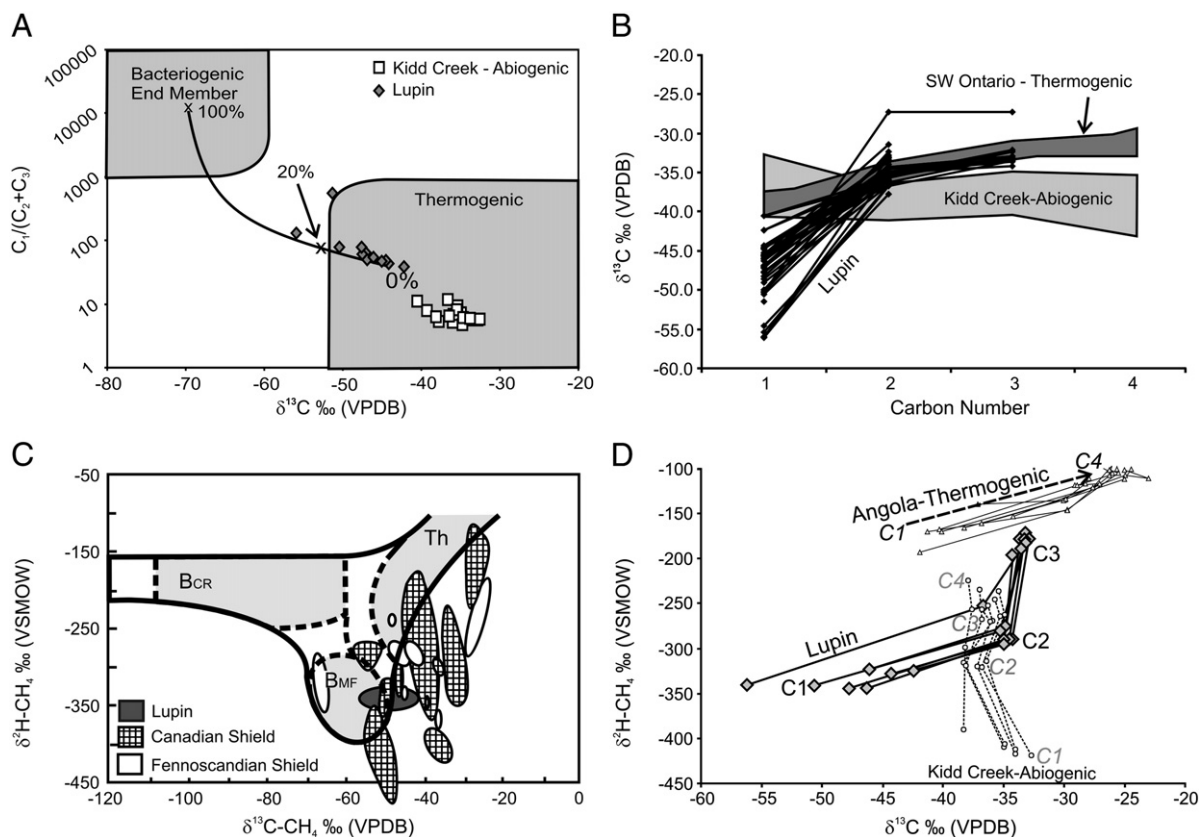


Fig. 7. Lupin gas relationships, compared with other sites, including Canadian and Fennoscandian Shield gases (Sherwood Lollar et al., 1993a,b) southwest Ontario natural gas fields (Sherwood Lollar et al., 1994), Angola gas fields (Prinzhofer and Huc, 1995), and the Kidd Creek mine (Sherwood Lollar et al., 2002). (A) $\delta^{13}C-CH_4$ versus $C_1/(C_2 + C_3)$ ratios. Lupin gases exhibit a typical mixing trend between thermogenic and bacteriogenic gases, (B) $\delta^{13}C$ ratios of individual hydrocarbons versus carbon number. The trend for Lupin gases is similar to sedimentary thermogenic gases rather than abiogenic shield gases. (C) Comparison of methane δ^2H and $\delta^{13}C$. Lightly shaded fields represent typical areas for bacterial carbonate reduction (B_{CR}), thermogenic associated gases (Th), and bacterial methyl-type fermentation (B_{MF}) (after Whiticar et al., 1986). In this plot, Lupin gases are similar to other gases sampled in the Canadian Shield and bacteriogenic methane formed via the methyl-fermentation pathway. (D). Relationship between $\delta^{13}C$ vs. δ^2H between C1, C2, C3.

did not support methanogenic bacteria (E_h : -189 to $+24$ mV, $O_2 < 2 \times 10^{-7}$ M) (Onstott et al., 2009; Stotler et al., 2009). Geochemical modeling also indicates that bacteriogenic methane reactions are less favored in less saline fluids (Onstott et al., 2009). However, the “bacteriogenic” end-member at Lupin was found in the borehole with the most dilute fluid. Methane concentration correlates with significantly over-pressured He and Ar concentrations (Fig. 3C and D), consistent with a geogenic source for these gases (e.g. Ballentine et al., 2002; Kipfer et al., 2002). Analyses of $^{14}C-CH_4$ (< 0.3 to 0.7 ± 0.1 pMC)

indicates methane formed from an older carbon pool than datable by the radiocarbon methodology (50 kyr).

3.3.2. Gas evolution

Due to the uncertainty regarding the gas origin and depleted δ^2H gas values, the potential for methane hydrate formation to affect the gas interpretation at this site was explored. It is generally accepted that very little $\delta^{13}C$ isotopic fractionation occurs as a result of gas hydrate formation, but until recently, very little information has been available regarding effects on δ^2H and molecular composition (Borowski et al., 1997; Milkov et al., 2004; Hatchikubo et al., 2007; Hatchikubo et al., 2009). Different crystalline methane hydrate structures have been recognized, which incorporate different gases. For instance, structure I hydrate (sI) incorporates only methane, while structure II hydrate (sII) may incorporate both methane and ethane (Sloan, 1998). The preferential incorporation of different gases into the hydrate structure does result in molecular gas composition fractionation (Milkov et al., 2004). Additionally, lab and field studies have shown that 2H depletion in both methane and ethane occurs in hydrate-bound gases compared to the original gases (Hatchikubo et al., 2007; Hatchikubo et al., 2009). At Lupin, δ^2H-C_1 and δ^2H-C_2 values (-350 to -330% and -330 to -230% VSMOW) were more negative than associated with previously described sedimentary thermogenic gases ($> -300\%$ and $> -200\%$ VSMOW), and although the $C_1/(C_2 + C_3)$ ratio was typical for thermogenic gas (< 100), hydrocarbons higher than C_3 were virtually undetectable. While experimentally derived hydrate- 2H fractionation is not large enough to account for the difference between typical thermogenic and Lupin gas δ^2H values, preferential incorporation of methane and ethane into

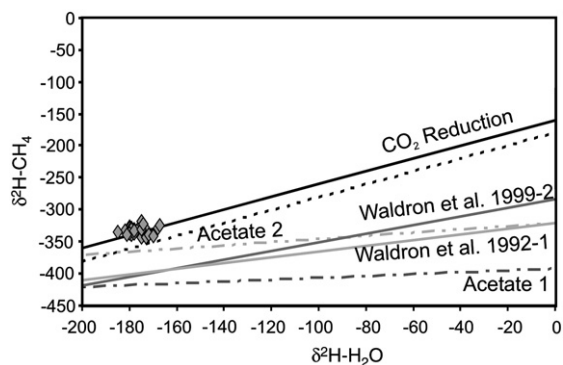


Fig. 8. Relationship between δ^2H-CH_4 and δ^2H-H_2O for Lupin gases. CO_2 reduction line from Schoell (1980) Acetate fermentation 1 line from (Jenden and Kaplan, 1986) Acetate fermentation 2 line from (Whiticar et al., 1986). The other two lines reflect shallow biogenic gas trends (Waldron et al., 1999).

sl and sll hydrate structures could account for the apparent loss of heavier hydrocarbons (C_3+). Depending on gas hydrate structure, the only unaffected genetic components typically utilized to determine gas origin at Lupin would be the carbon isotopic compositions and propane hydrogen isotope compositions. It is thus likely that methane hydrate formation affected Lupin gas molecular and isotopic compositions.

However, further consideration of the depleted δ^2H gas values is required, as methane hydrate formation cannot explain the magnitude of δ^2H depletion from other thermogenic gases. Although carbon isotopic compositions indicated mixing between at least two different methane sources, there was relatively little variation in δ^2H-CH_4 values. δ^2H-CH_4 values are expected to be different for gases of different origins, due to different hydrogen sources and fractionation pathways (e.g. Schimmelmann et al., 2006). Thus it was unlikely that the final δ^2H values for both of the two CH_4 end-members (“bacteriogenic” and “thermogenic”) would be the same or very similar, indicating some alternative process must have affected the δ^2H-CH_4 values. Hydrogen isotopic fractionation during primary production is controlled by δ^2H-H_2O or $-H_2$ values and/or metabolic processes (Whiticar, 1996, 1999). During thermogenic methane formation, hydrogen molecules are derived from the decarboxylated organic material (e.g. Schoell, 1980; Whiticar, 1996). 2H depletion in crystalline abiotic gases is attributed to polymerization reactions (Sherwood Lollar et al., 2002, 2006). From field data, primary fields have been determined where δ^2H values for thermogenic gases have a range between -275 and -100% (VSMOW), for bacteriogenic methane: between -250 and -170% (VSMOW) for the carbonate reduction pathway, and between -531 and -250% (VSMOW) for the methyl-type fermentation pathway, and for abiogenic gases between -430 and -230% (Whiticar, 1999; McCollom and Seewald, 2007). However, these fields are incomplete; depleted δ^2H values (-416 to -380% VSMOW) associated with carbonate reduction were recently observed in methane emissions from Arctic lakes (Chanton et al., 2006; Walter et al., 2008). Further, empirical relationships used to determine bacteriogenic methanogenesis pathways are only useful in some situations, they do not properly account for mixing of multiple hydrogen sources and products, resulting in a non-unique solution (Conrad, 2005; Sessions and Hayes, 2005). Further, independent of the gas evolution pathway, methane δ^2H values may change considerably (150% in one experiment) if only the hydrogen concentration changes (Burke, 1993).

Hydrogen isotope exchange also may occur over geologic times greater than >350 Ma (Sessions et al., 2004). If the Lupin gas originated during metamorphic events, sufficient time would have elapsed for hydrogen isotope exchange to occur, possibly accounting for the similar hydrogen isotope values between mixed gas pathways. Given the lack of H_2 in the gas phase at Lupin (Onstott et al., 2009), exchange with H_2 is unlikely, thus H_2O is the only remaining major hydrogen source. However, the CH_4-H_2O fractionation factor ($\alpha_{O,W}$) is 0.692 (Sessions et al., 2004); considering the current δ^2H value for Lupin groundwater ($\sim -180\%$ VSMOW), δ^2H-CH_4 values should be enriched by $\sim 225\%$ (VSMOW) compared to observed values; a more enriched δ^2H-H_2O value would result in even greater enrichment in δ^2H-CH_4 values. Therefore, hydrogen isotope exchange over geologic time likely does not account for the depleted δ^2H values.

In summary, a scenario to satisfactorily explain the depleted δ^2H values was not identified, thus gas origins and evolution remain uncertain. The gas composition, carbon isotopic composition, relative fractionation of carbon and hydrogen isotopes between the different gas species, and geologic history indicate gas of a thermogenic origin, but an abiogenic origin cannot be ruled out due to the presence of depleted δ^2H isotopic values. It is suggested that several genetic and post-genetic processes, including methane hydrate formation, contributed to the mixed gas composition observed at the site. Regardless

of gas origin, there were no indications of modern methanogenic processes.

4. Conclusions

This first investigation of the occurrence, phase, and origin of alkanes in crystalline rocks under thick permafrost conditions indicates the gases are present naturally within fractures as gas hydrates. Dewatering operations by the mine served to depressurize the nearby rock mass, destabilizing some methane hydrate. Gas concentrations are lower than typical for gas hydrate formation, likely because the concentrations obtained were averages for entire boreholes. Borehole video surveys indicated gas was present only in certain fractures, where concentrations would be higher than the borehole average. Noble gas data and pressure measurements support a conclusion that de-watering depressurized the area near the mine, resulting in gas hydrate dissociation.

The origin of gases sampled at Lupin was difficult to determine conclusively. It is suggested the geochemical trends are evidence of thermogenic gas mixed with microbial gas. However the data indicates that methanogenesis was not a modern process. The site has considerable metasedimentary and higher-grade metamorphic rocks that were originally organic-rich mud rock. Thermogenic gas genesis would be tied to metamorphic events, suggesting gas has been present between 1.81 and 2.68 Ga. Thermogenic gas remnants may also occur at other shield locations with a similar geologic setting. Although it is likely methane hydrate formation affected gas molecular and hydrogen isotope composition, the depleted δ^2H values were inconsistent with a thermogenic gas origin, but not readily explained by other processes.

Although subsurface conditions have changed significantly over the last 120 ka, climate modeling suggests that no possibility existed for large-scale methane releases at the Lupin site during this period. Rather, during glacial advance, gas hydrate stability fields increased in size. Thus, gases trapped at Lupin during glacial cycles were not an active part of the recent global carbon cycle. Paleo-subglacial gas hydrate formation likely was not restricted to crystalline shield locations, and the potential for hydrate formation during glaciation should be investigated in previously glaciated sedimentary basin gas reservoirs, such as the Williston, Illinois, and Michigan basins in North America.

The presence of gas hydrates over extended periods of time may significantly affect the possibility for subglacial recharge, particularly in crystalline rock, where flow pathways are limited. This would affect long-term stability scenarios for subsurface nuclear waste disposal in northern countries. If sufficient gas were present, gas hydrate formation would reduce subsurface permeability and porosity, similar to ice formation. This would then limit flow and hydraulic pathways, which would restrict the potential for subglacial recharge. Depending on the context, paleo-groundwater flow models and reconstructions need to account for the potential for gas hydrate formation to more accurately depict subglacial and glacial meltwater recharge scenarios.

Acknowledgements

This research is part of a highly collaborative research program, supported by (in alphabetical order) the Geological Survey of Finland; NASA Astrobiology Institute, USA; Natural Sciences and Engineering Research Council (NSERC) of Canada; Nirex Ltd, UK; Nuclear Waste Management Organization (NWMO), Canada; Ontario Power Generation (OPG), Canada (through the Deep Geologic Repository Technical Program, Nuclear Waste Management Division); Posiva Oy, Finland; and Svensk Kärnbränslehantering AB (SKB), Sweden. Echo Bay Mines and Kinross Gold graciously provided access to the Lupin mine. We appreciated assistance from Adam Johnson and the support of the

Lupin employees. Comments from two anonymous reviewers improved the manuscript.

Appendix A. Supplementary Data

Supplementary data associated with this article can be found, in the online version, at doi:10.1016/j.epsl.2010.05.024.

References

- Ballentine, C.J., Burgess, R., Marty, B., 2002. Tracing fluid origin, transport and interaction in the crust. *Rev. Mineral. Geochem.* 47, 481–538.
- Borowski, W.S., Paull, C.K., Ussler III, W., 1997. Carbon cycling within the upper methanogenic zone of continental rise sediments: an example from the methane-rich sediments overlying the Blake Ridge gas hydrate deposits. *Mar. Chem.* 57, 299–311.
- Burke Jr., R.A., 1993. Possible influence of hydrogen concentration on microbial methane stable hydrogen isotopic composition. *Chemosphere* 26, 55–67.
- Burt, T.P., Williams, P.J., 1976. Hydraulic conductivity in frozen soils. *Earth Surf. Process.* 1, 349–360.
- Chanton, J.P., Fields, D., Mines, M.E., 2006. Controls on the hydrogen isotopic composition of biogenic methane from high latitude terrestrial wetlands. *J. Geophys. Res.* 111, G04004. doi:10.1029/2005JG000134.
- Claypool, G.E., Threlkeld, C.N., Mankiewicz, P.N., Arthur, M.A., Anderson, T.F., 1985. Isotopic composition of interstitial fluids and origin of methane in slope sediment of the Middle America Trench, Deep Sea Drilling Project, Leg 84. In: von Huene, R., Aubouin, J., et al. (Eds.), *Initial Reports, DSDP 84*, pp. 683–691.
- Collett, T.S., Ginsburg, G.D., 1998. Gas hydrates in the Messoyakha Gas Field of the West Siberian Basin – a re-examination of the geologic evidence. *Int. J. Offshore Polar Eng.* 8, 22–29.
- Collett, T.S., Kvenvolden, K.A., Magoon, L.B., 1990. Characterization of hydrocarbon gas within the stratigraphic interval of gas-hydrate stability on the North Slope of Alaska, U.S.A. *Appl. Geochem.* 5, 279–287.
- Conrad, R., 2005. Quantification of methanogenic pathways using stable carbon isotope signatures: a review and a proposal. *Org. Geochem.* 36, 739–752.
- Dallimore, S.R., Collett, T.S., 1995. Intraperafrost gas hydrates from a deep core hole in the Mackenzie Delta, Northwest Territories, Canada. *Geology* 23 (6), 527–530.
- Dallimore, S.R., Collett, T.S. (Eds.), 2005. Scientific results from the Mallik 2002 Gas Hydrate Production Research Well Program, Mackenzie Delta, Northwest Territories, Canada: Geological Survey of Canada Bulletin, 585.
- Dallimore, S.R., Uchida, T., Collett, T.S. (Eds.), 1999. Scientific results from JAPEX/JNOC/GSC Mallik 2L-38 Gas Hydrate Research Well, Mackenzie Delta, Northwest Territories, Canada: Geological Survey of Canada Bulletin, 544.
- Des Marais, D.J., Donchin, J.H., Nehring, N.L., Truesdell, A.H., 1981. Molecular carbon isotopic evidence for the origin of geothermal hydrocarbons. *Nature* 292, 826–828.
- Dickens, G.R., Paull, C.K., Wallace, P., and the ODP Leg 164 Scientific Party, 1997. Direct measurement of in situ methane quantities in a large gas-hydrate reservoir. *Nature* 385, 427–428.
- Dutkiewicz, A., Ridley, J., Buick, R., 2003. Oil-bearing CO₂–CH₄–H₂O fluid inclusions: oil survival since the Palaeoproterozoic after high temperature entrapment. *Chem. Geol.* 194, 51–79.
- Geusebroek, P.A., Duke, N.A., 2004. An update on the geology of the Lupin Gold Mine, Nunavut, Canada. *Explor. Mining Geol.* 13, 1–13.
- Goodarzi, F., Eckstrand, O.R., Snowdon, L., Williamson, B., Stasiuk, L.D., 1992. Thermal metamorphism of bitumen in Archean rocks by ultramafic volcanic flows. *Int. J. Coal Geol.* 20, 165–178.
- Greene, S., 2005. Noble gases of the Canadian Shield from the Lupin and Con mines, Canada, as indicators of deep groundwater flow dynamics and residence time. M.Sc. Thesis, University of Ottawa, Ottawa, Ontario.
- Hachikubo, A., Manakov, A., Kida, M., Krylov, A., Sakagami, H., Minami, H., Takahashi, N., Shoji, H., Kalmaychkov, G., Poort, J., 2009. Model of formation of double structure gas hydrates in Lake Baikal based on isotopic data. *Geophys. Res. Lett.* 36, L18504. doi:10.1029/2009GL039805 (5p).
- Hatchikubo, A., Kosaka, T., Kida, M., Krylov, A., Sakagami, H., Minami, H., Takahashi, N., Shoji, H., 2007. Isotopic fractionation of methane and ethane hydrates between gas and hydrate phases. *Geophys. Res. Lett.* 34, L21502. doi:10.1029/2007GL030557 (5p).
- Hesse, R., Harrison, W.E., 1981. Gas hydrates (clathrates) causing pore-water freshening and oxygen-isotope fractionation in deep-water sedimentary sections of terrigenous continental margins. *Earth Planet. Sci. Lett.* 55, 453–462.
- Hinrichs, K.-U., Hayes, J.M., Bach, W., Spivack, A.J., Hmelo, L.R., Holm, N.G., Johnson, C.G., Sylva, S.P., 2006. Biological formation of ethane and propane in the deep marine subsurface. *Proc. Natl Acad. Sci. USA* 103, 14684–14689.
- James, A.T., 1983. Correlation of natural gas by use of carbon isotopic distribution between hydrocarbon components. *AAPG Bull.* 67, 1176–1191.
- Jenden, P.D., Kaplan, I.R., 1986. Comparison of microbial gases from the Middle America Trench and Scripps Submarine Canyon: implications for the origin of natural gas. *Appl. Geochem.* 1, 631–646.
- Kennett, J.P., Cannariato, K.G., Hendy, I.L., Behl, R.J., 2000. Carbon isotopic evidence for methane hydrate instability during Quaternary Interstadials. *Science* 288, 128–133.
- King, J.E., Davis, W.J., Relf, C., Avery, R.W., 1988. Deformation and plutonism in the Western Contwoyot Lake map area, central Slave province, District of Mackenzie, N.W.T. *Geol. Surv. Can. Pap.* 88-1C, 161–176.
- Kipfer, R., Aeschbach-Hertig, W., Peeters, F., Stute, M., 2002. Noble gases in lakes and ground waters. *Rev. Mineral. Geochem.* 47, 615–700.
- Kleinberg, R.L., Flaum, C., Griffin, D.D., Brewer, P.G., Malby, G.E., Peltzer, E.T., Yesinowski, J.P., 2003. Deep sea NMR: methane hydrate growth habit in porous media and its relationship to hydraulic permeability, deposit accumulation, and submarine slope stability. *J. Geophys. Res.* 108 (B10), 2508. doi:10.1029/2003JB002389.
- Kusky, T.M., 1989. Accretion of the Archean Slave Province. *Geol.* 17, 63–67.
- Kvenvolden, K.A., Lorenson, T.D., 2001. The global occurrence of natural gas hydrate. In: Paull, C.K., Dillon, W.P. (Eds.), *Natural Gas Hydrates: Occurrence, Distribution, and Dynamics: AGU Monograph Series*, 124, pp. 3–18.
- Lemieux, J.-M., Sudicky, E.A., Peltier, W.R., Tarasov, L., 2008a. Dynamics of groundwater recharge and seepage over the Canadian landscape during the Wisconsinian glaciation. *J. Geophys. Res.* 113, F01011. doi:10.1029/2007JF000838.
- Lemieux, J.-M., Sudicky, E.A., Peltier, W.R., Tarasov, L., 2008b. Simulating the impact of glaciations on continental groundwater flow systems: 1. Relevant processes and model formulation. *J. Geophys. Res.* 113, F03017. doi:10.1029/2007JF000928.
- Lemieux, J.-M., Sudicky, E.A., Peltier, W.R., Tarasov, L., 2008c. Simulating the impact of glaciations on continental groundwater flow systems: 2. Model application to the Wisconsinian glaciation over the Canadian landscape. *J. Geophys. Res.* 113, F03018. doi:10.1029/2007JF000929.
- Majorowicz, J.A., Osadetz, K.A., 2001. Gas hydrate distribution and volume in Canada. *AAPG Bull.* 85 (7), 1211–1230.
- Mazor, E., 1972. Paleotemperatures and other hydrological parameters deduced from noble gases dissolved in groundwaters; Jordan Rift Valley, Israel. *Geochem. Cosmochim. Acta* 36, 1321–1336.
- McCullom, T.M., Seewald, J.S., 2001. A reassessment of the potential for reduction of dissolved CO₂ to hydrocarbons during serpentinization of olivine. *Geochim. Cosmochim. Acta* 65, 3769–3778.
- McCullom, T.M., Seewald, J.S., 2006. Carbon isotope composition of organic compounds produced by abiotic synthesis under hydrothermal conditions. *Earth Planet. Sci. Lett.* 243, 74–84.
- McCullom, T.M., Seewald, J.S., 2007. Abiotic synthesis of organic compounds in deep-sea hydrothermal environments. *Chem. Rev.* 107, 382–401.
- Melezhik, V.A., Fallick, A.E., Filippov, M.M., Larsen, O., 1999. Karelian shungite – an indication of 2.0-Ga-old metamorphosed oil-shale and generation of petroleum: geology, lithology, and geochemistry. *Earth Sci. Rev.* 47, 1–40.
- Milkov, A.V., Claypool, G.E., Lee, Y.-J., Xu, W., Dickens, G.R., Borowski, W.S., 2003. In situ methane concentrations at Hydrate Ridge, offshore Oregon; new constraints on the global gas hydrate inventory. *Geology* 31, 833–836.
- Milkov, A.V., Claypool, G.E., Lee, Y.-J., Torres, M.E., Borowski, W.S., Tomaru, H., Sassen, R., Long, P.E., and ODP Leg 204 Scientific Party, 2004. Ethane enrichment and propane depletion in subsurface gases indicate gas hydrate occurrence in marine sediments at southern Hydrate Ridge, offshore Oregon. *Org. Geochem.* 35, 1067–1080.
- Mossman, D.J., Nagy, B., Davis, D.W., 1993. Hydrothermal alteration of organic matter in uranium ores, Elliot Lake, Canada: implications for selected organic-rich deposits. *Geochim. Cosmochim. Acta* 57, 3251–3259.
- Natural Resources Canada, 1995. Canada – Permafrost. The National Atlas of Canada, 5th Edition. (MCR 4177).
- Nisbet, E.G., 1990. The end of the ice age. *Can. J. Earth Sci.* 27, 148–157.
- Onstott, T.C., McGown, D.J., Bakermans, C., Ruskeeniem, T., Ahonen, L., Telling, J., Soffientino, B., Piffner, S.M., Sherwood-Lollar, B., Frappe, S., Stotler, R., Johnson, E.J., Vishnivetskaya, T.A., Rothmel, R., Pratt, L.M., 2009. Microbial communities in subpermafrost saline fracture water at the Lupin Au Mine, Nunavut, Canada. *Microb. Ecol.* 58, 786–807. doi:10.1007/s00248-009-9553-5.
- Oremland, R.S., Whiticar, M.J., Strohmaier, F.E., Kiene, R.P., 1988. Bacterial ethane formation from reduced, ethylated sulfur compounds in anoxic sediments. *Geochim. Cosmochim. Acta* 52, 1895–1904.
- Person, M., McIntosh, J., Bense, V., Remenda, V.H., 2007. Pleistocene hydrology of North America: the role of ice sheets in reorganizing groundwater flow systems. *Rev. Geophys.* 45. doi:10.1029/2006RG000206 RG3007.
- Petersilie, I.A., Sørensen, H., 1970. Hydrocarbon gases and bituminous substances in rocks from the Ilímaussaq alkaline intrusion, south Greenland. *Cont. Mineral. Ilímaussaq* 18, 59–76.
- Potter, J., Rankin, A.H., Treloar, P.J., 2004. Abiogenic Fischer–Tropsch synthesis of hydrocarbons in alkaline igneous rocks; fluid inclusion, textural and isotopic evidence from Lovozero complex, N.W. Russia. *Lithos* 75, 311–330.
- Prinzhofer, A.A., Huc, A.Y., 1995. Genetic and post-genetic molecular and isotopic fractionations in natural gases. *Chem. Geol.* 126, 281–290.
- Sackett, W.M., Nakaparskin, S., Dalrymple, S., 1970. Carbon isotope effects in methane production by thermal cracking. In: Hobson, G.D., Speers, G.C. (Eds.), *Advances in Organic Geochemistry*. Pergamon Press, pp. 37–53.
- Schimmelmann, A., Sessions, A.L., Mastalerz, M., 2006. Hydrogen isotopic (D/H) composition of organic matter during diagenesis and thermal maturation. *Annu. Rev. Earth Planet. Sci.* 34, 501–533.
- Schoell, M., 1980. The hydrogen and carbon isotopic composition of methane from natural gases of various origins. *Geochim. Cosmochim. Acta* 44, 649–661.
- Sessions, A.L., Hayes, J.M., 2005. Calculation of hydrogen isotope fractionations in biogeochemical systems. *Geochim. Cosmochim. Acta* 69, 593–597.
- Sessions, A.L., Sylva, S.P., Summons, R.E., Hayes, J.M., 2004. Isotopic exchange of carbon-bound hydrogen over geologic timescales. *Geochim. Cosmochim. Acta* 68, 1545–1559.
- Sherwood Lollar, B., Frappe, S.K., Fritz, P., Macko, S.A., Welhan, J.A., Blomqvist, R., Lahermo, P.W., 1993a. Evidence for bacterially generated hydrocarbon gas in Canadian Shield and Fennoscandian Shield rocks. *Geochim. Cosmochim. Acta* 57, 5073–5086.

- Sherwood Lollar, B., Frappe, S.K., Weise, S.M., Fritz, P., Macko, S.A., Welhan, J.A., 1993b. Abiogenic methanogenesis in crystalline rocks. *Geochim. Cosmochim. Acta* 57, 5087–5097.
- Sherwood Lollar, B., Weise, S.M., Frappe, S.K., Barker, J.F., 1994. Isotopic constraints on the migration of hydrocarbon and helium gases of southwestern Ontario. *Bull. Can. Petrol. Geol.* 42, 283–295.
- Sherwood Lollar, B., Lacrampe-Couloume, T.B., Ward, J.A., Slater, G.F., Lacrampe-Couloume, G.L., 2002. Abiogenic formation of alkanes in the Earth's crust as a minor source for global hydrocarbon reservoirs. *Nature* 416, 522–524.
- Sherwood Lollar, B., Lacrampe-Couloume, G., Slater, G.F., Ward, J., Moser, D.P., Gihring, T.M., Lin, L.H., Onstott, T.C., 2006. Unraveling abiogenic and biogenic sources of methane in the Earth's deep subsurface. *Chem. Geol.* 226, 328–339.
- Sloan, E.D., 1998. *Clathrate Hydrates of Natural Gases*. Marcel Dekker Inc.
- Stotler, R.L., Frappe, S.K., Ruskeeniemi, T., Ahonen, L., Onstott, T.C., Hobbs, M.Y., 2009. Hydrogeochemistry of groundwaters in and below the base of thick permafrost at Lupin, Nunavut, Canada. *J. Hydrol.* 373, 80–95.
- Taran, Y.A., Kliger, G.A., Sevastianov, V.S., 2007. Carbon isotope effects in the open-system Fischer–Tropsch synthesis. *Geochim. Cosmochim. Acta* 71, 4474–4487.
- Tarasov, L., Peltier, W.R., 2005. Arctic freshwater forcing of the Younger Dryas cold reversal. *Nature* 435, 662–665.
- Tarasov, L., Peltier, W.R., 2007. The co-evolution of continental ice cover and permafrost extent over the last glacial–interglacial cycle in North America. *J. Geophys. Res. Earth Surf.* 112 (F02S08). doi:10.1029/2006JF000661.
- Therrien, R., McLaren, R.G., Sudicky, E.A., Panday, S.M., 2007. *Hydrosphere: A Three-dimensional Numerical Model Describing Fully-integrated Subsurface and Surface Flow and Solute Transport*. Groundwater Simulations Group, Waterloo, ON, Canada.
- Tréhu, A.M., Long, P.E., Torres, M.E., Bohrmann, G., Rack, F.R., Collett, T.S., Goldberg, D.S., Milkov, A.V., Riedel, M., Schultheiss, P., Bangs, N.L., Barr, S.R., Borowski, W.S., Claypool, G.E., Delwiche, M.E., Dickens, G.R., Gracia, E., Guerin, G., Holland, M., Johnson, J.E., Lee, Y.-J., Liu, C.-S., Su, X., Teichert, B., Tomaru, H., Vanneste, M., Watanabe, M., Weinberger, J.L., 2004. Three-dimensional distribution of gas hydrate beneath southern Hydrate Ridge: constraints from ODP Leg 204. *Earth Planet. Sci. Lett.* 222, 845–862.
- Voytov, G.I., 1991. Chemical and carbon-isotope fluctuations in free gases (gas jets) in the Khibiny. *Geokhimiya* 6, 769–780.
- Waldron, S., Lansdown, J.M., Scott, E.M., Fallick, A.E., Hall, A.J., 1999. The global influence of the hydrogen isotope composition of water on that of bacteriogenic methane from shallow freshwater environments. *Geochim. Cosmochim. Acta* 63, 2237–2245.
- Walter, K.M., Chanton, J.P., Chapin III, F.S., Schuur, E.A.G., Zimov, S.A., 2008. Methane production and bubble emissions from arctic lakes – isotopic implications for source pathways and ages. *J. Geophys. Res.* 113 (G00A08). doi:10.1029/2007JG000569 (16p).
- Weitemeyer, K.A., Buffett, B.A., 2006. Accumulation and release of methane from clathrates below the Laurentide and Cordilleran ice sheets. *Glob. Planet. Change* 53, 176–187.
- Whiticar, M.J., 1996. Stable isotope geochemistry of coals, humic kerogens, and related natural gases. *Int. J. Coal Geol.* 32, 191–215.
- Whiticar, M.J., 1999. Carbon and hydrogen isotope systematics of bacterial formation and oxidation of methane. *Chem. Geol.* 161, 291–314.
- Whiticar, M.J., Faber, E., Schoell, M., 1986. Biogenic methane formation in marine and freshwater environments: CO₂ reduction vs. acetate fermentation – isotope evidence. *Geochim. Cosmochim. Acta* 50, 693–709.
- Wright, J.F., Taylor, A.E., Dallimore, S.R., Nixon, F.M., 1999. Estimating in situ gas hydrate saturation from core temperature observations, JAPEX/JNOC/GSC Mallik 2L-38 gas hydrate research well. In: Dallimore, S.R., Uchida, T., Collett, T.S. (Eds.), *Scientific Results from JAPEX/JNOC/GSC Mallik 2L-38 Gas Hydrate Research Well, Mackenzie Delta, Northwest Territories, Canada*: Geol. Surv. Canada Bull., 544, pp. 101–108.
- Yakushev, V.S., Chuvilin, E.M., 2000. Natural gas and gas hydrate accumulations within permafrost in Russia. *Cold Reg. Sci. Technol.* 31, 189–197.
- Youngman, M.J., 1989. *Dissolved gases and radioelements in groundwaters*. PhD Thesis, The British Library, West Yorkshire. 422p.
- Zhou, Y., Castaldi, M.J., Yegulalp, T.M., 2009. Experimental investigation of methane gas production from methane hydrate. *Ind. Eng. Chem. Res.* 48, 3142–3149.